

## Periodic corrugation on dynamic fracture surface in brittle bulk metallic glass

X. K. Xi, D. Q. Zhao, M. X. Pan, and W. H. Wang<sup>a)</sup>

*Institute of Physics, Chinese Academy of Sciences, Beijing 100080, China*

Y. Wu

*Department of Physics and Astronomy, University of North Carolina, Chapel Hill, North Carolina 27599-3255*

J. J. Lewandowski

*Department of Materials Science and Engineering, Case Western Reserve University, 10900 Euclid Avenue, Cleveland, Ohio 44106*

(Received 21 August 2006; accepted 17 September 2006; published online 31 October 2006)

Dynamic crack propagation in a model brittle bulk metallic glass (BMG) is studied. Contrary to other brittle glassy materials, the authors find nanometer scale out-of-plane periodic corrugations along the crack surface of the BMG. The nanoscale periodicity remains nearly constant at different loading rates. An interpretation is presented to explain the evolution and the periodic coalescence of the nanometer scale cavities along the crack surface. The observation sheds light on the origin of dynamic fracture surface roughening in brittle materials and could be generally applicable to brittle materials. © 2006 American Institute of Physics. [DOI: 10.1063/1.2374688]

The fracture in brittle glasses has a complicated morphology, and the moving crack results in three-dimensional (3D) surface roughness, acoustic wave, crack oscillating and branching which do not exist in the classical theories of crack propagation.<sup>1-4</sup> Intensive works have been carried out to study the fracture surface roughening phenomena in order to uncover the mechanisms governing the dynamics of crack propagation.<sup>1-4</sup> Dynamic propagating cracks produce a release of fracture energy by acoustic emission in the form of elastic waves<sup>2,3</sup> that propagate both into the bulk (such as shear waves) as well as along the newly formed fracture surface (Rayleigh waves).<sup>5</sup> The waves as well as their reflected waves by the sample boundaries interfere with the stress fields of the crack tip and result in a transient increase or decrease of the crack tip stress intensity. Consequently, the moving crack will alternately propagate and arrest, leaving undulations on the fracture surface.<sup>1,6</sup> The interaction of the crack with material inhomogeneity also generates the waves with a wavelength of micrometers, millimeters or higher scales.<sup>1-4</sup> However, the origin of the fracture surface corrugations and the energy dissipation mechanism remain unclear.<sup>1,2,7-9</sup>

Previous dynamic fracture studies focused on brittle glassy polymers, oxide glasses, and polymer gels.<sup>1,2,10</sup> The recently developed brittle bulk metallic glasses (BMGs) have been used as another kind of model material to study the features of propagating cracks in brittle glassy materials.<sup>11</sup> The atomic-scale disorder in metallic glasses has significant structural difference from that of oxide glasses, glassy polymers, or gels. In this sense, the fracture behaviors of the brittle BMG might be distinguished from those of other brittle glasses.<sup>12</sup> On the other hand, the fracture surface of conducting BMGs can be conveniently investigated on nanometer scale using a high resolution scanning electron microscopy (HRSEM). This provides much higher spatial resolution about crack propagation, which is especially important

for the early stages of the fracture surface roughening.

In this work, we report the dynamic morphology along the fracture surface of a brittle BMG using the HRSEM and atomic force microscopy (AFM) with suitable control strategies. The nanoscale out-of-plane periodic corrugations on the fracture surface of the BMG are observed, and the reason for the periodic roughening is discussed. The results might provide an insight on the origin of dynamic fracture surface roughening in brittle materials.

The 5-mm-diameter cylindrical Mg<sub>65</sub>Cu<sub>25</sub>Tb<sub>10</sub> BMG with a notch in the center of the specimen was prepared using a diamond saw satisfying plane-strain conditions. The notch fracture toughness  $K_c$  of the BMG is about  $2.0 \pm 0.2$  MPa  $\sqrt{m}$ , which approaches the ideal brittle behavior associated with silicate glasses with  $K_{IC} \sim 0.02-0.8$  MPa  $\sqrt{m}$  at room temperature.<sup>13</sup> Annealing far below the glass transition temperature  $T_g$  was performed to eliminate possible residual stress. The fracture surfaces were prepared by three point bending fracture of single edge notched samples on an MTS 810 servo hydraulic testing machine. We used a cross head speed of 1 cm/min up to a certain load rate to prevent spalling at ambient conditions (the cross head speed change from 1 to 10 mm/min). Load and load point displacement were monitored during the test (see details in Ref. 14). The newly created fracture surfaces were examined using a Philips XL30 SEM with a resolution of 1.5 nm and a Digital NanoScope IIIa D-3000 AFM.

The notch specimens three point bent to fracture have the distinct mist and mirror zones as previously reported.<sup>11</sup> The unique feature along the crack surface is the nearly constant periodicity of the undulations in the mirror zone (see Fig. 1). More structural details between these lines are shown in Fig. 1(b) at higher magnification. The undulations become straight and parallel far from the notch edge ( $\sim 1$  mm) indicating that the crack velocity changes very slowly and the local crack front tip is straight.<sup>15</sup> Furthermore, the straight crack front configuration is stable to isolated perturbations as shown in Fig. 1(a), where the crack front passes a flaw in the BMG matrix (as indicated) but shows no significant influ-

<sup>a)</sup> Author to whom correspondence should be addressed; electronic mail: whw@aphy.iphy.ac.cn

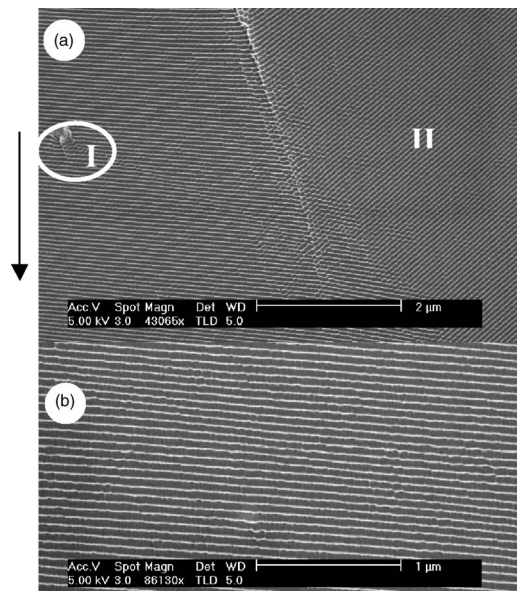


FIG. 1. Periodic corrugations along the crack surfaces of Mg-based BMG far ahead of the notch. (a) SEM micrograph showing two-line (band) systems interacting with each other and the presence of a flaw on the fracture surface (zone I), (b) is a higher magnification of zone II in (a). An arrow shows the crack propagation direction.

ence on the periodicity. In addition, the 3D view of an AFM scan of this region (not shown) shows that the shape of these roughness oscillations exhibits a peak-to-peak matching when compared with the matched crack surface. The corrugations are also observed along the crack surface of the relaxed glassy specimen (annealed below  $T_g$  at 375 K for  $\sim 30$  min) and the spacing is nearly the same. This excludes the effect of possible residual stress on the formation of the corrugations. In contrast, in the fracture surface features of a crystallized specimen (annealed at 465 K above crystallization temperature) no periodic lines are formed, and the feature of intergranular fracture is observed.

AFM was applied to further characterize the structural evolution of the fracture surface with increasing distance from the notch site. Figure 2(a) is the optical microscopy examination of the fractured specimen and gives an overview to locate the high magnification micrographs of AFM. Figure 2(b) shows a top view AFM image of zone *b* in Fig. 2(a) and dominant cavities on  $\sim 90$  nm with a disordered distribution are observed. This structure is formed when the dynamic crack propagates, and a large number of voids nucleate and grow rapidly into damage cavities at the crack tip. The material between the damage cavities necks down, demonstrating a local plastic instability.<sup>16</sup>

Figure 2(c) illustrates the periodic variations along the crack propagation direction in zone *c*. This shows that the velocity has already become oscillatory well before the roughness transition while the fracture surface is still optically smooth and planar. The dominant feature in this zone is the ordered assembly of the cavities. The ordered assembly of the cavities forms the periodic corrugations. Figure 2(d) shows similar periodic corrugations, however, with a slightly wider periodicity, possibly indicating that oscillatory cracks propagate with relatively higher velocity.<sup>17</sup> Figure 2(e) shows that the hackle zone *e* is rougher than the other zones. Figures 2(b)–2(d) show that the damage cavities on the fracture surface grow from small to large, from disordered to

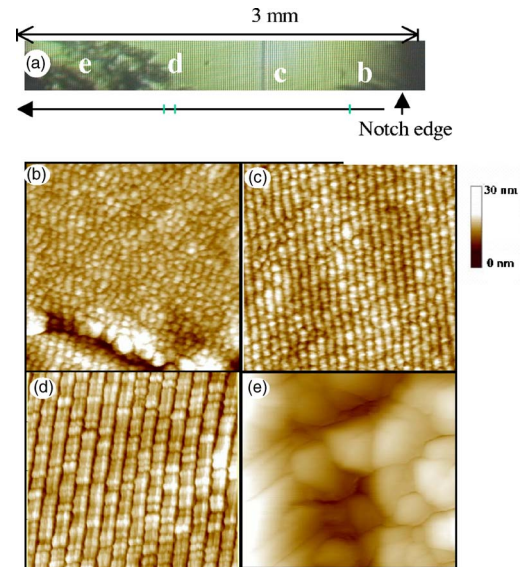


FIG. 2. (Color online) Dynamic evolution of fracture surfaces of  $\text{Mg}_{65}\text{Cu}_{25}\text{Tb}_{10}$  BMG. (a) Optical microscopy overview of the dynamic fracture surface of the Mg-based BMG. AFM top view: (b) zone *b*, (c) zone *c*, (d) zone *d*, and (e) zone *e*. Image size:  $1 \times 1 \mu\text{m}^2$ . The rms roughness on the fracture surfaces for zones *b*, *c*, *d*, and *e* are 0.75, 1.37, 2.21, and 74.93 nm, respectively. Arrows show the crack propagation direction.

ordered arrangement, and to disordered arrangement again with the crack propagation in the brittle BMG. Figures 2(d) and 2(e) also show a sharp crack surface roughness transition. The variations of root-mean-square (rms) roughness quantified by AFM on  $1 \times 1 \mu\text{m}^2$  surfaces for zones *b*, *c*, *d*, and *e* are 0.75, 1.37, 2.21, and 74.93 nm, respectively. The rms evolution in the mirror region from *b* to *d* corresponds to the periodicity of the corrugations and crack velocity with slight fluctuations. However, the markedly increase (nearly two orders of magnitude) of the fracture roughness between mirror zone edge *d* and hackle zone *e* demonstrates the sharply increased fracture energy dissipation at crack tip, resulting from the multicracking mechanism.<sup>9</sup> The surface rms variations further suggests that the velocity is not the driving factor in determining the periodicity since the velocity variations along the crack front are not expected to be significant; however, stress state variations are quite significant due to changes in the constraint along the moving crack front.

We note that at lower loading rates or with sharper notch the mirror region spreads over almost the entire fracture surface. As the loading rate is increased, the mirror region becomes progressively restricted and the mist zone or hackle zone is increased. However, the structural features remain unchanged, and the spacing of the corrugations in the mirror region remains nearly constant under the loading rate range (the cross head speed changes from 1 to 10 mm/min), and there is no essential influence of the loading rate on the periodicity.

In general, crack velocity  $V_c$  ( $V_c = f\lambda$ , where  $\lambda$  is the wavelength and  $f$  is the sound frequency) is about  $0.3\text{--}0.6V_R$  in dynamically steady state for brittle amorphous materials.<sup>17–19</sup> The Rayleigh wave speed  $V_R \approx 0.9225V_s$ , where  $V_s$  is shear wave velocity. For the BMG,  $V_s$  is  $\sim 2300$  m/s, and the Poisson ratio  $\nu$  is 0.313.<sup>20</sup> Thus, the  $f$  of frequency crack velocity oscillating the brittle BMG is estimated to be on the order of  $\sim 10^4$  MHz, far beyond the reasonable acoustic emission frequency range.<sup>21</sup> Therefore, the

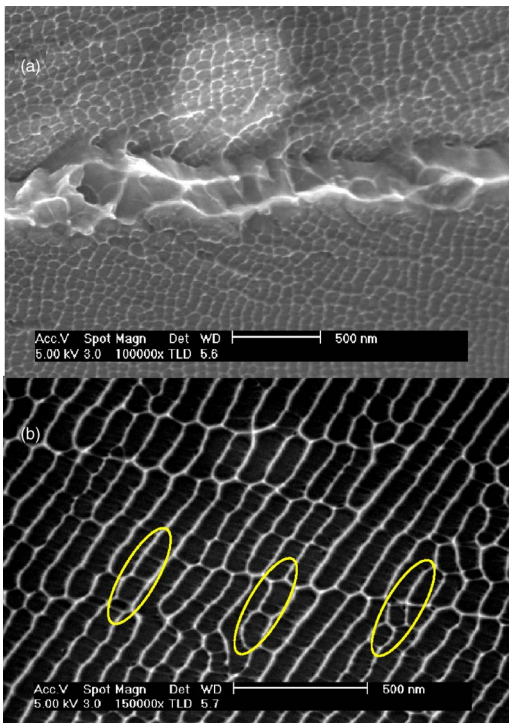


FIG. 3. (Color online) HRSEM images of the fracture surface of the BMG. (a) Disordered distribution of the damage cavities on the fracture surface when the bent fracture load rate is very low. [The damage cavity structure has also been confirmed by AFM (Ref. 11)]. (b) The assembly process of the cavities on the fracture surface between zones *b* and *c* (closer to *a*) in Fig. 2(a). Self-assembly of damage cavities along the fracture surface can be clearly observed on the marked areas in (b).

observed periodic corrugations in the BMG cannot be attributed to the Wallner lines.<sup>1</sup> The crack front tip instability was predicted recently by out-of-plane crack front waves which is assumed to be due to long-range elastic effects causing the dynamic stress transfer along the crack front.<sup>2</sup> The observed phenomenon in the BMG is not the crack front waves either, because the periodic perturbations cannot occur in BMG with homogenous microstructure and without periodic structural asperities.

Figure 3(a) shows the nanometer scale damage cavities (about 100 nm) on the fracture surface prepared by the three point bending fracture with very low load rate (the cross head speed is 0.1 mm/min), which demonstrates a blunted plane crack and the propagation of the fracture front via the coalescence of the damage cavities.<sup>11</sup> The high tensile stress at the crack front can lead to the growth/coalescence of the cavities along the crack surface.<sup>11,18,22</sup> The significant elastic stress field fluctuations in the fracture process zone and thus result in the directional preference of the damage cavity. At very low crack velocities the effects can be strongly suppressed.<sup>2</sup> For the fast propagating crack, various fracture elements operating simultaneously tend to a condition in which the material in the oncoming crack path is permeated by periodic stress fields. The formation of the periodic corrugations along the crack surface demonstrates such coalescence of the damage cavities.

Figure 3(b) clearly shows the coalescence of the cavities along the crack surface. Previous observations also demonstrate that a certain cavity density is required to form a periodic corrugation pattern.<sup>18,23</sup> This indicates that assembly oc-

curs only when damage cavities are close enough and within each other's elastic influence range. Consequently, a directional stress field and the size of damage cavities are two significant aspects in the assembling process. This result explains the existence of a characteristic cavity size for periodic corrugation formation in our study. The threshold of characteristic cavity size for periodic corrugation formation is experimentally estimated to be about 100 nm. It is reasonable to expect that if the fracture toughness is lowered or the fracture strength is enhanced, the damage cavities will be lowered to some degree, i.e., close to the periodicity of elastic waves, and then the undulations should appear.

From the energetic point of view, when cavities accumulate along certain directions under certain stress field, extra energy dissipation of the fast moving crack should be balanced with energy transfer along the dynamic steady-state crack front. Previous studies indicate that corrugation periodicity of brittle glasses is material specific and correlates with properties such as fracture surface energy. And such effects become significant when the fracture surface energy decreases to a threshold.<sup>18,23</sup> Periodic corrugations have been observed on the fracture surface of different brittle materials, and the periodicity ranges from millimeter scale in polymer gels,<sup>10</sup> micrometer in glassy polymers,<sup>18,24</sup> to nanometer scale in brittle BMGs. The similarity in various brittle amorphous materials with much different properties implies that the basic processes operate during the dynamic fracture of brittle materials—there exists universality to the dynamics of oscillating crack in fast fracture of brittle amorphous materials.

Support from the NSFC (Grant Nos. 10328408 and 50321101) is acknowledged.

<sup>1</sup>D. Bonamy and K. Ravi-Chandar, Phys. Rev. Lett. **93**, 099602 (2004); **91**, 235502 (2003).

<sup>2</sup>E. Sharon, G. Cohen, and J. Fineberg, Phys. Rev. Lett. **88**, 085503 (2002).

<sup>3</sup>J. E. Field, Contemp. Phys. **12**, 1 (1971).

<sup>4</sup>S. Ramanathan and D. S. Fisher, Phys. Rev. Lett. **79**, 877 (1997).

<sup>5</sup>A. M. Fitzgerald, T. W. Kenny, and R. H. Dauskardt, Exp. Mech. **43**, 317 (2003).

<sup>6</sup>T. A. Michalske and V. D. Frechette, Int. J. Fract. **17**, 251 (1981).

<sup>7</sup>E. Bouchaud, J. Mech. Phys. Solids **50**, 1703 (2002).

<sup>8</sup>N. H. Tran and R. N. Lamb, Chem. Phys. Lett. **391**, 385 (2004).

<sup>9</sup>B. N. Cox, J. Mech. Phys. Solids **53**, 565 (2005).

<sup>10</sup>Y. Tanaka, J. Phys. Soc. Jpn. **65**, 2349 (1996); D. Bonn, Science **280**, 265 (1998).

<sup>11</sup>X. K. Xi, D. Q. Zhao, M. X. Pan, W. H. Wang, Y. Wu, and J. J. Lewandowski, Phys. Rev. Lett. **94**, 125510 (2005); X. K. Xi, Ph.D. thesis, CAS, 2005.

<sup>12</sup>L. B. Freund, *Dynamic Fracture Mechanics* (Cambridge University Press, Cambridge, UK, 1990).

<sup>13</sup>J. J. Lewandowski, W. H. Wang, and A. L. Greer, Philos. Mag. Lett. **85**, 77 (2005).

<sup>14</sup>P. Lowhaphandu and J. J. Lewandowski, Scr. Mater. **38**, 1811 (1998).

<sup>15</sup>B. W. Payne and A. Ball, Philos. Mag. **34**, 917 (1976).

<sup>16</sup>K. M. Flores and R. H. Dauskardt, J. Mater. Res. **14**, 638 (1999).

<sup>17</sup>W. G. Knauss and K. Ravi-Chandar, Int. J. Fract. **27**, 127 (1985).

<sup>18</sup>K. Ravi-Chandar and B. Yang, J. Mech. Phys. Solids **45**, 535 (1997).

<sup>19</sup>J. R. Rice, Y. Ben-Zion, and K. S. Kim, J. Mech. Phys. Solids **42**, 813 (1994).

<sup>20</sup>W. H. Wang, C. Dong, and C. H. Shek, Mater. Sci. Eng., R. **44**, 45 (2004).

<sup>21</sup>S. P. Gross, Phys. Rev. Lett. **71**, 3162 (1993).

<sup>22</sup>N. Eliaz, Metall. Mater. Trans. A **31**, 1085 (2000).

<sup>23</sup>R. P. Kusy and D. T. Turner, Polymer **18**, 391 (1977).

<sup>24</sup>K. Friedrich, J. Mater. Sci. Lett. **12**, 640 (1977).